

THE REALIZATION OF THE DEFINITION OF THE METRE AT INRIM

*M. Zucco*¹, *M. Bisi*², and *P. Cordiale*³

¹Istituto Nazionale di Ricerca Metrologica, INRIM, Torino, Italy, m.zucco@inrim.it

²Istituto Nazionale di Ricerca Metrologica, INRIM, Torino, Italy, m.bisi@inrim.it

³Istituto Nazionale di Ricerca Metrologica, INRIM, Torino, Italy, p.cordiale@inrim.it

Abstract: In this paper we present the traceability chain for the calibration of the frequency of laser standards that realize the definition of the metre at the National Institute of Metrological Research (INRIM) in Italy in accordance with the *mise en pratique* issued by the CIPM. We describe the way our femtosecond laser frequency combs are referenced to the SI second and the new research activity on the production and testing of iodine cells.

Keywords: metrology, lasers, measurement standards, iodine spectroscopy, wavelength standards.

1. INTRODUCTION

INRIM is the National Institute of Metrological Research in Italy having the task of maintaining standards, undertaking their international comparisons and in general providing measurements traceability to the SI. The traceability chain for the realization of the definition of the metre at INRIM is presented in Fig. 1, where the traceability to the second is provided in the laboratory of the metre through a RF link and an optical link. Different laser standards are maintained which realize the metre in accordance with the *mise en pratique* (MeP) of the definition of the metre by means of one of the recommended radiations listed in the Recommendation issued by the CIPM [1], [2]. There are two femtosecond laser frequency combs (FLFC) operating at INRIM at two different spectral regions. Laser standards are calibrated on a regular basis with FLFCs or with primary laser standards. The laser radiation could be sent to the laboratory of the metre through optical link without the need to displace the laser. Laser standards are then used in interferometers and in other standards to disseminate the metre to dimensional metrology.

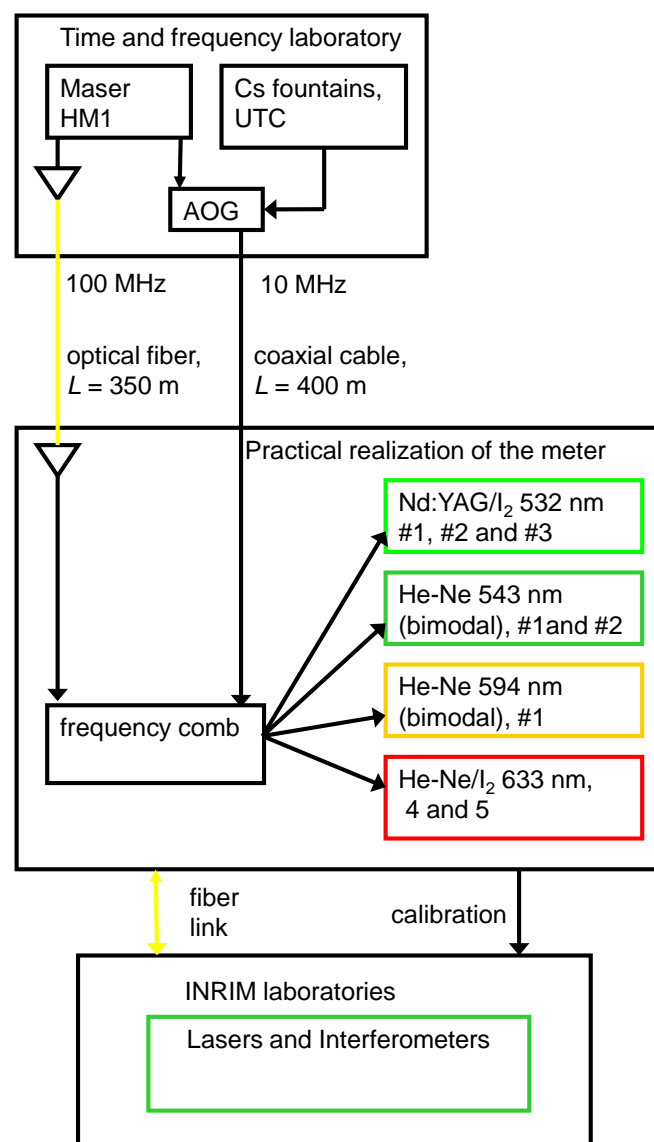


Fig. 1. Scheme of the traceability chain for the realization of the definition at INRIM.

2. TRACEABILITY TO THE SECOND

As is seen in Fig. 1, time base is provided to the laboratory of the metre through two different routes. One time base is provided by a 10 MHz signal referred to UTC(IT), generated by an Active Hydrogen Maser steered to UTC by means of an Auxiliary Output Generator (AOG) with BIPM circular T and/or direct measurement by INRIM Cs atomic fountain that regularly participates to TAI generation. The time base is delivered by a 400 m coaxial cable not compensated. The uncertainty associated to the time base is $3 \cdot 10^{-14}$ (k=2). The second way to provide the time base to the laboratory is by means of a 100 MHz signal generated directly from the Hydrogen Maser and delivered to the laboratory of the metre by modulating the amplitude of a telecom laser at 1.5 μm and sending the radiation through a 350 m long fiber. A receiver in the laboratory demodulates the 100 MHz and divides it by ten to generate the 10 MHz time base. The correction and the uncertainty is provided monthly by the BIPM circular T. The fiber link is not phase compensated, but there is a project to compensate it by using a fiber stretcher. As indicated in Fig. 2 a), the 10 MHz time is used to provide directly the reference to all the instruments for frequency generation / measurement (modulators, frequency counters, synthesizers). The reference signal at 100 MHz in Fig. 2b), delivered with the optical link in Fig. 1, is multiplied to 1 GHz to provide directly the reference to the FLFC repetition rate PLLs for applications where the final stability is an issue.

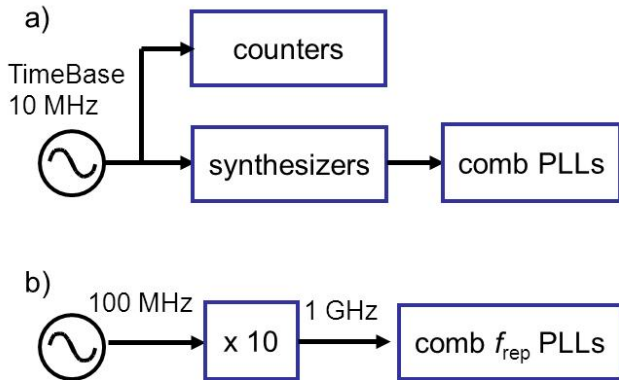


Fig. 2. The different implementation of the 10 MHz (a) and 100 MHz (b) time base.

In Fig. 3, the single sideband phase noise $L(f)$ of the RF and optical link output at 10 MHz and the phase noise of the optical link directly at 100 MHz (scaled to 10 MHz). From the graph, it is evident that the divider by ten adds phase noise above 100 Hz. The phase noise is measured with respect to a low noise quartz oscillator.

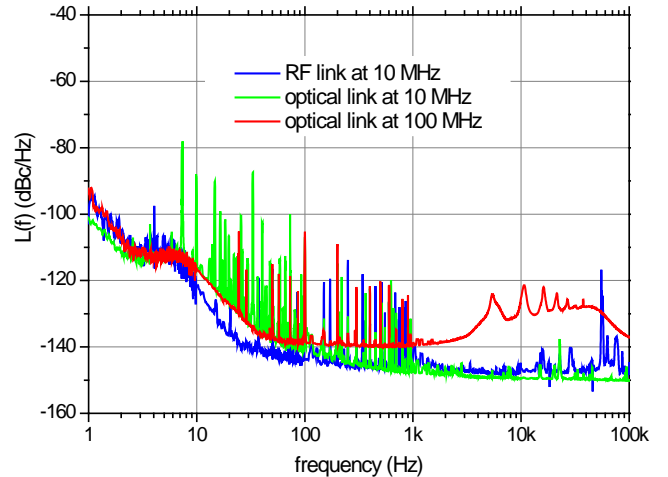


Fig. 3. The single sideband phase noise $L(f)$ scaled at 10 MHz of the RF and optical link measured with respect to a low noise quartz oscillator.

As a conclusion, for applications where the final stability is not an issue, the 10 MHz signal is used as time base for the synthesizers generating the local oscillator for the offset f_o and repetition rate f_{rep} PLL. The stability is limited by the synthesizer and the attainable Allan deviation is estimated to be $6 \cdot 10^{-13}$ measured in a 1 Hz bandwidth. Whereas for applications where it is important to reach the ultimate stability limit of the Hydrogen Maser, the low noise 1 GHz in Fig. 2 is used and the attainable Allan deviation is estimated to be $2 \cdot 10^{-13}$ measured in a 1 Hz bandwidth.

3. THE OPTICAL COMBS AT INRIM

At INRIM two different FLFCs, based on two different set-ups, are maintained. One comb is based on a commercial femtosecond laser with a Ti:Sa crystal which generates 35 fs pulses with a repetition rate of about 1 GHz with a carrier at 810 nm, and a power of about 0.9 W when pumped with 5.4 W generated by a frequency-doubled Nd:YVO₄ laser. The spectrum is broadened by means of a photonic crystal to the range 500 nm – 1064 nm to measure the offset frequency f_o . The component at 1064 nm is selected by a dichroic mirror and doubled by a PPKTP crystal, the doubled component at 532 nm is mixed with the component at 532 nm to generate the offset f_o beatnote which is controlled by changing the pump laser power. Repetition rate f_{rep} is controlled by changing the laser cavity length. The entire system is contained in a $76 \times 44 \times 22 \text{ cm}^3$ aluminum box. The second FLFC generates the optical comb in the region 1000 nm – 2000 nm and is based on full commercial Er-doped fiber laser having a repetition rate of about 250 MHz. Repetition rate is measured and controlled by filtering the 4th harmonic at 1 GHz and using one the two schemes in Fig. 2 according to the needs.

4. LASER STANDARDS

Laser standards shown in Fig. 1 are mainly used at INRIM for interferometry and dimensional applications.

They are all traceable to the metre and to the second through the route represented in Fig. 1 where the uncertainty is $3 \cdot 10^{-14}$. The workhorse of all the laser standards is the He-Ne lasers at 633 nm, which can be locked to the laser emission profile (for example with the bimodal technique) or to iodine hyperfine transitions. We have two primary standards (INRIM4 and INRIM5) operating at INRIM based on He-Ne lasers locked to the f component of the 11-5 R(127) transition of iodine at 633 nm. The primary standard INRIM4 has been compared on a regular basis and participated to BIPM.L- K10 key comparison in 1995, see Fig. 4, where key comparison reference value was BIPM-4 laser and the measurand was the difference between the average frequency of the components d, e, f, and g in the R(127) 11-5 line as obtained by matrix measurements [3]. Two measurements were carried out with the BIPM comb of the laser INRIM4 locked to the f component, one in 2003 and one in 2006, the last one as a part of BIPM.L-K11 key comparison [4]. Since 2010 absolute measurements of INRIM4 frequency have been carried out with INRIM combs, two results are reported in Fig 4.

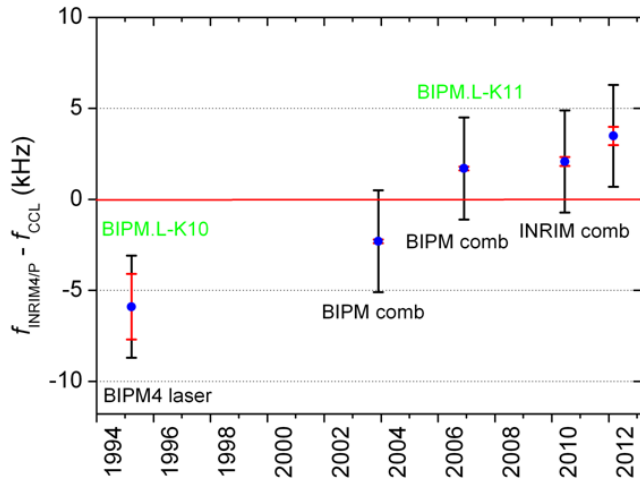


Fig. 4. Primary standard INRIM4 has been compared on a regular basis. The result is reported as the frequency difference of the f component of the 11-5 R(127) transition of $^{127}\text{I}_2$ with respect to the recommended values by the CIPM.

In Fig 4, results are reported with two different error bars, Red error bars represent the uncertainties in the frequency measurement and include the statistical dispersion of the measurement and the time base uncertainty. Black error bars are the uncertainties of laser frequency propagated from the setting of the laser operating conditions to the values recommended by the CIPM [1], [2]. The operating conditions are the intracavity laser power, the modulation width, the iodine cell cold finger temperature, the iodine cell wall temperature. Other parameters to be taken into accounts are the electronics offset and the beam alignment.

When the operating parameters cannot be set exactly at the value reported in the *MeP*, it is possible to calculate the frequency that the laser would have at the *MeP* set points by correcting the measured frequency through the sensitivity coefficients. The sensitivity coefficients are measured by

measuring the frequency shift by changing one operating parameters each time. The sensitivity coefficients of primary standard INRIM4, as reported in report [4], are presented in Table 1. The uncertainty budget of INRIM4 taking into account the contribution of uncertainty coming from the operating parameters and from the sensitivity coefficients is in Table 2.

Parameter	Sensitivity Coefficient Value	Uncertainty	Unit
Modulation width	-11.1	0.2	kHz/MHz
Iodine pressure	-8.5	0.1	kHz/Pa
Power (output)	-0.059	0.008	kHz/ μW
Cell wall temperature	0.06	0.06	kHz/ $^{\circ}\text{C}$

Table 1. The sensitivity coefficients and associated uncertainty of primary standard INRIM4, as reported in report [4].

Source	Value	Unit
Laser power	0.12	kHz
Modulation width	2.22	kHz
Iodine cold finger temperature	1.36	kHz
Cell wall temp	0.42	kHz
Electronic offset	1.00	kHz
Total	2.82	kHz

Table 2. Uncertainty budget of primary standard INRIM4 with the contribution from the operating parameters and sensitivity coefficients.

Three different Nd:YAG laser standards, frequency-doubled at 532 nm, are operating at INRIM. Two are based on the recommended line, a_{10} component, R(56) 32-0 transition $^{127}\text{I}_2$, using the modulation transfer technique. Nd:YAG laser standards have a certain number of advantages when compared to He-Ne/ I_2 lasers, like an unmodulated output with higher optical power and a shorter wavelength, making it more suitable for interferometric applications. In Fig. 5, a series of measurements of prototype INRIM1 carried out with INRIM FLFC. The first two measurements are carried out on the 532 nm output using Ti:Sa FLFC, whereas the last measurement is carried out on the 1064 nm output using the fiber FLFC.

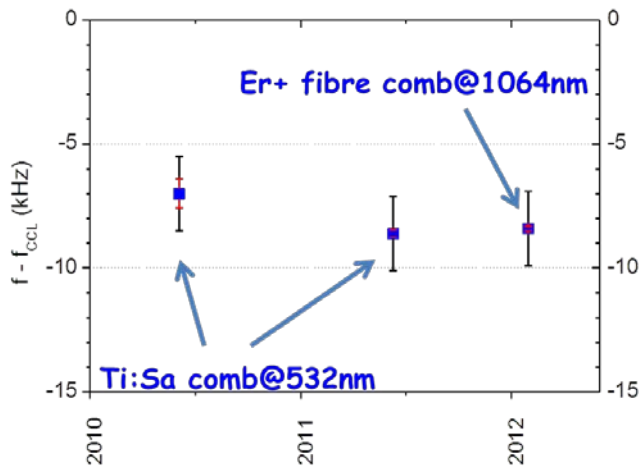


Fig. 5. A series of measurements of the frequency of INRIM1 Nd:YAG laser locked to the a^{10} component, R(56) 32-0 transition $^{127}\text{I}_2$.

In Fig. 6, the Allan deviation of the beatnote between the output at 1064 nm of the locked Nd:YAG laser and the fiber FLFC when the repetition rate is phase locked to the low noise 1 GHz in Fig. 2b). For gate time lower than 10 s, the stability reaches the Hydrogen Maser noise limit.

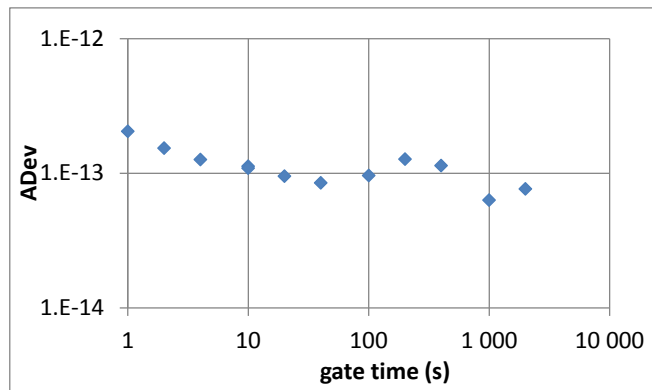


Fig. 6. Allan deviation of the beatnote between the output at 1064 nm of the locked Nd:YAG laser and the fiber FLFC when the repetition rate is phase locked to the low noise 1 GHz in Fig. 2b). For gate time lower than 10 s, the stability attains the Hydrogen Maser noise floor.

5. IODINE CELL PRODUCTION

Iodine cells production and testing started at INRIM (formerly IMGC-CNR) premises in the early '70s, this activity has been resumed in the last year. In Fig. 7 a detail of the vacuum system with four quartz cells ready to be filled with iodine vapor.

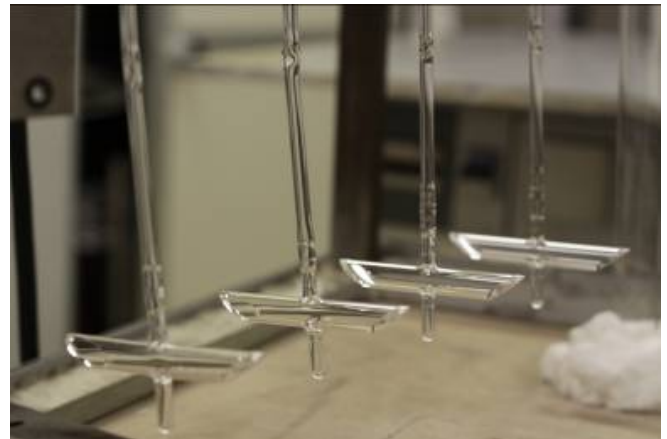


Fig. 7. A detail of the vacuum system with four cells ready to be filled with iodine vapor.

Iodine transitions represent a dense grid of reference lines in the visible and near infrared electromagnetic spectrum, and they provide a useful calibration tool for spectroscopy research and for laser standards. Saturated iodine gas is contained in quartz or pyrex cells whose pressure is set by controlling the cold finger temperature. The cells have different geometries and size and are implemented in laser standards using different techniques. As an example, 10 cm long cells with windows at the Brewster angle, like the one in Fig. 8, and cold finger at 15 °C are inserted inside the laser cavity of He-Ne lasers.

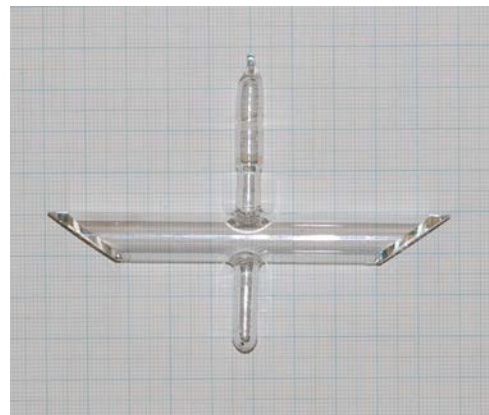


Fig. 8. A cell filled with saturated iodine gas to be inserted in a He-Ne laser. The length is 10 cm and the windows are at the Brewster angle. The bottom side-arm is used as the cold finger to set the gas pressure inside the cell. The top side-arm is the pyrex sealing tip.

Much longer cells, with quasi parallel windows and cold finger at much lower temperature, are used externally to the laser cavity, like in Nd:YAG laser standards at 532 nm. Moreover, when the transition frequency goes towards the dissociation limit, the natural line widths decreases at a faster rate than that for the line strength [5] and therefore these iodine based standards are good candidates for having even higher stability, compactness and portability. Nevertheless, the reproducibility of the iodine laser standard [6] is likely to be limited by the iodine cell quality. In fact,

the presence of foreign gases in the cell causes pressure broadening and shifts of the iodine transition frequency and therefore of the laser standards. For this reason, we characterize the iodine cell quality with two different techniques. In the heterodyne technique the cell is inserted in the corresponding laser system (intracavity for the He-Ne laser at 633 nm, extracavity for the Nd:YAG laser at 532 nm). The laser cavity is realigned and the operating parameters are set to the *MeP* value, then when the laser cavity is thermalized, the laser is locked to the recommended transition and the laser frequency is measured by comparing it with our laser standards which are measured on a regular basis with respect to our combs. In this way, it is possible to give the frequency shift with respect to the recommended value in the *MeP* as a measurement of the quality of the cell. Unfortunately, this technique is time consuming since it requires at least one day to align the cavity and thermally stabilize it and is limited by the uncertainty in the laser systems. The second technique is based on the laser induced fluorescence LIF [7]: a multimode Ar⁺ laser emitting at 501.7 nm with line-width of about 5 GHz excites the transition R(26) 62-0 of the system B³Π - X Σ of the iodine molecule. The LIF intensity is measured as a function of iodine pressure in the cell. When the iodine pressure is constant, the fluorescence intensity is proportional to the total effective decay time, by increasing the iodine pressure the decay time is decreased by self quenching: excited molecules decays by non-radiative mechanisms. When other gases are present in the cell, the decay time is further decreased and the LIF intensity follows the model of the normalized Stern-Volmert equation

$$\frac{I_o}{I_F} = K_o \frac{1}{p_I} + L_o \quad (1)$$

where I_F is the LIF intensity, I_o a normalizing parameter, p_I the iodine pressure, L_o a constant depending on iodine parameters. K_o is the parameter dependent on the foreign gas partial pressure. In Fig. 9, the graph of the LIF measurement of cell INRIM#2 (similar to the cell in Fig. 8), the result of the measurement gives $K_o = (1.35 + 0.02)$ Pa, with the uncertainty $u = 0.02$ Pa coming from the least square estimation. According to statistics collected in [7], this K_o value corresponds to a high quality iodine cell, in fact the measured frequency shift is $\delta f_{\text{CCL}} = (-4.2 \pm 4.0)$ kHz, where the uncertainty of 4.0 kHz comes from the quadratic sum of the uncertainties of the two lasers used for the frequency measurement.

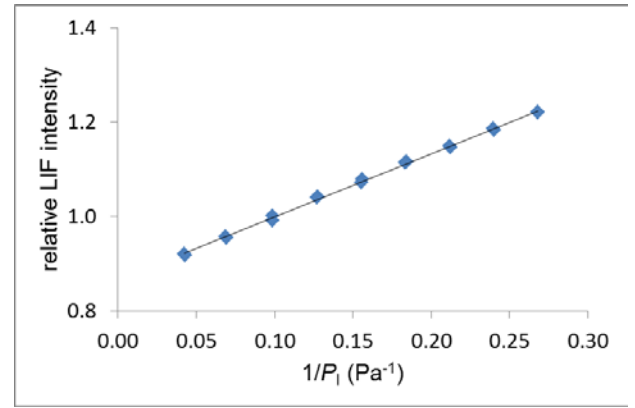


Fig. 9. The result of the LIF measurement of cell INRIM#2, the result of the measurement gives $K_o = (1.35 + 0.02)$ Pa.

7. REFERENCES

- [1] T.J. Quinn, "Practical realization of the definition of the metre, including recommended radiations of other optical frequency standards (2001)", *Metrologia*, 40, 103-133, 2003.
- [2] <http://www.bipm.org/en/committees/cc/ccl/mep.html>
- [3] H. Darnedde, W. R. C. Rowley, F. Bertinnetto, Y. Millerieux, H. Haitjema, S. Wetzels, H. Pirée, E. Prieto, M. Mar Pérez, B. Vaucher, A. Chartier and J.-M. Chartier, "International comparisons of He-Ne lasers stabilized with 12712 at $\lambda = 633$ nm (July 1993 to September 1995). Part IV: Comparison of Western European lasers at $\lambda = 633$ nm", *Metrologia*, 36, 199-206, 1999.
- [4] L. Robertsson, R. Felder, F. Bertinnetto, P. Cordiale, J.-P. Wallerand, H. Suh, H. Hussein, R. Hamid, E. Sahin, "Results from the CII-2006 campaign at the BIPM of the BIPM.L-K11 ongoing key comparison", *Metrologia*, 44, Tech. Suppl., 04003, 2007
- [5] J W.-Y. Cheng, L. Chen, T. Hyun Yoon, J. L. Hall, and J. Ye, "Sub-Doppler molecular-iodine transitions near the dissociation limit (523–498 nm)," *Opt. Lett.*, 27, 571-573, 2002.
- [6] J.-M. Chartier, A. Chartier, "I₂-stabilized 633-nm He-Ne lasers: 25 years of international comparisons", *Proc. SPIE* 4269, 123-132, 2001.
- [7] S Fredin-Picard, "A Study of Contamination in ¹²⁷I₂ Cells Using Laser-Induced Fluorescence" *Metrologia*, 26, 235-244, 1989